**SUPPLEMENTARY INFORMATION**

**Role of mammalian Mre11 in classical and alternative non-homologous end joining**
Anyong Xie, Amy Kwok and Ralph Scully

**Supplementary Figure 1**

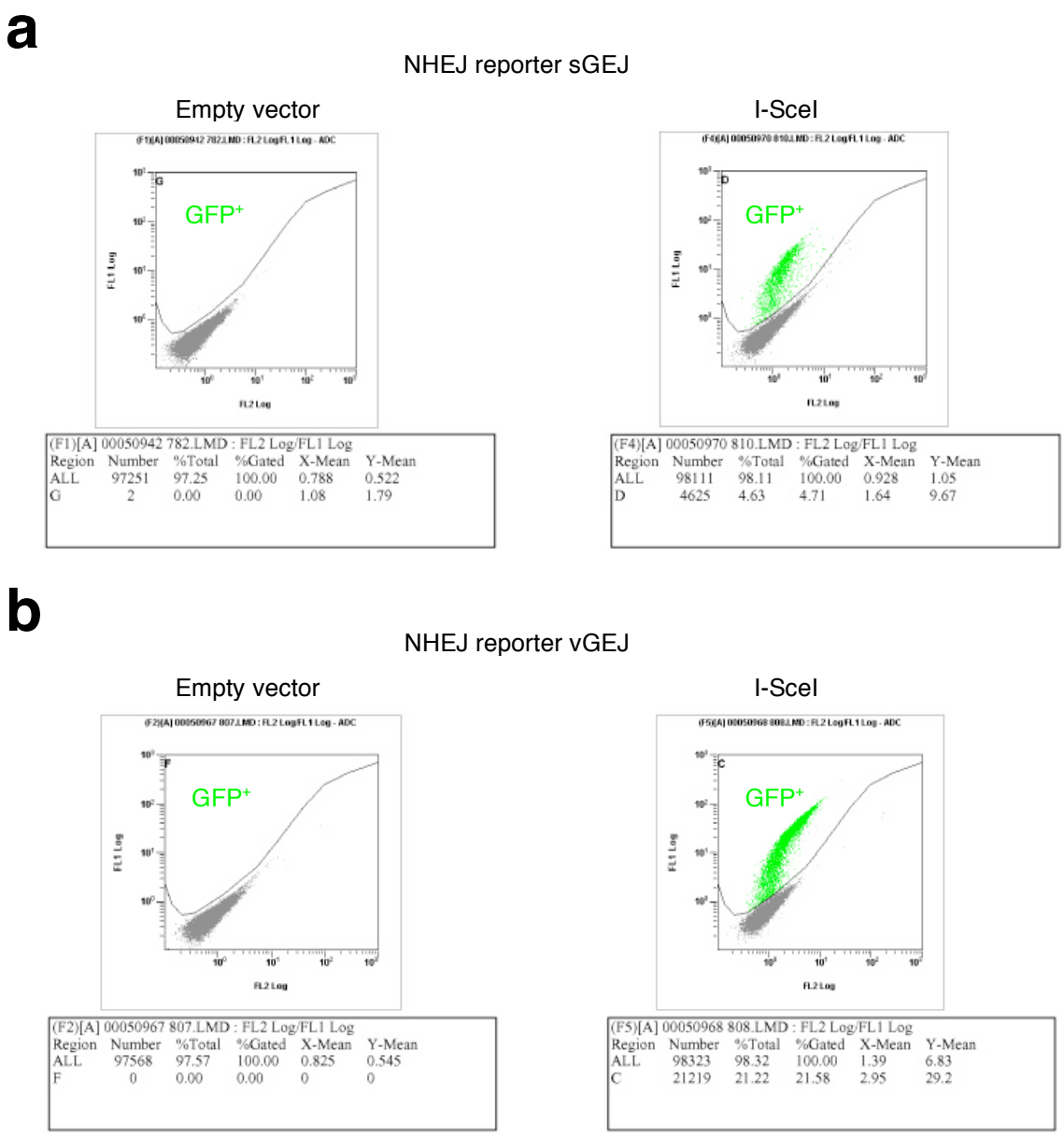


**Supplementary Figure 1** Induction of GFP$^+$ cells by I-SceI. FACS analysis was performed 3 days after transfection of *Xrcc4*$^{flox/flox}$ sGEJ (**a**) or vGEJ reporter mouse ES cells (**b**) with empty vector or with an I-SceI plasmid. GFP$^+$ cells lie above the diagonal, percentages as indicated. FL1 Log: green fluorescence. FL2 Log: red fluorescence.

**Supplementary Figure 2**

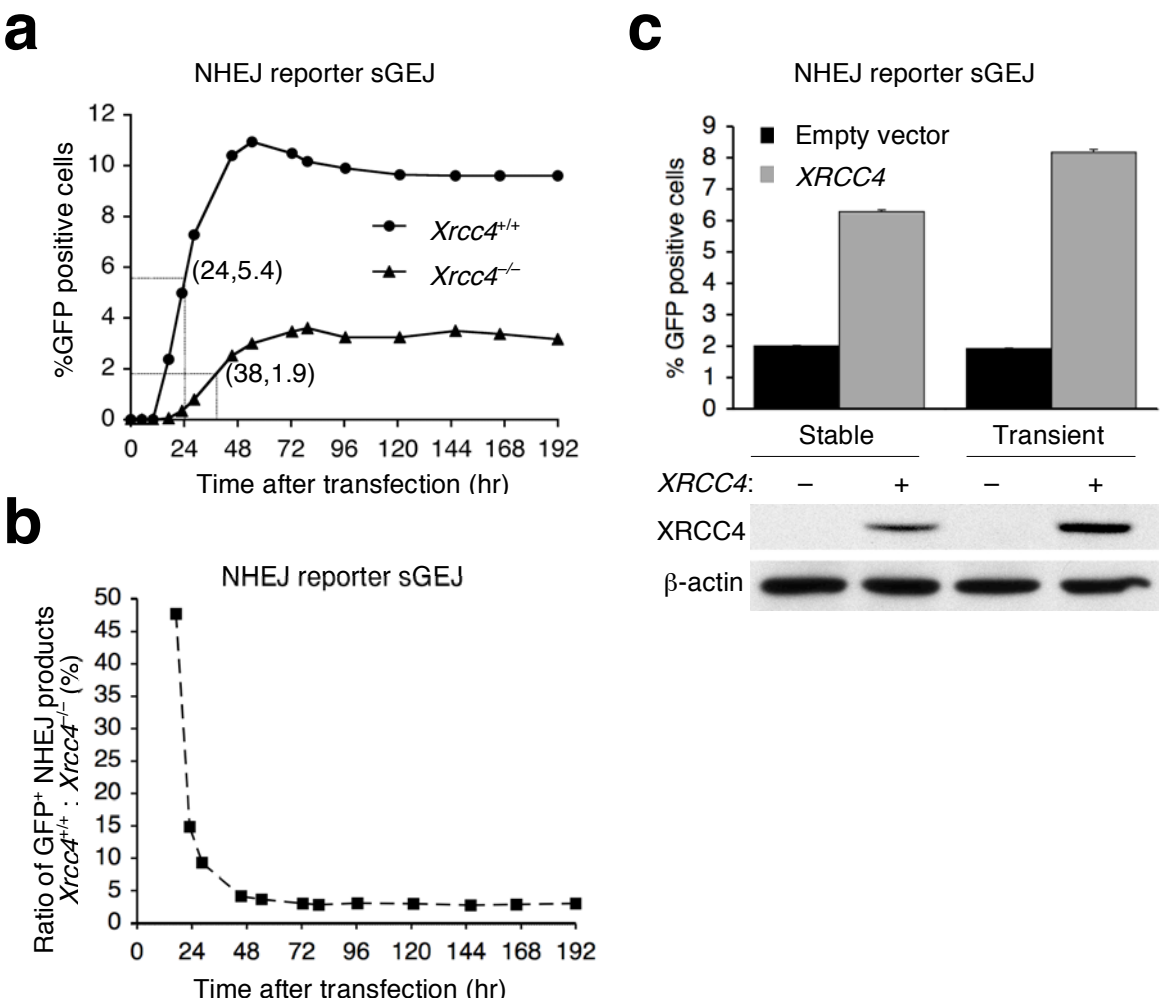


**Supplementary Figure 2** Alternative *Xrcc4*-independent NHEJ acts more slowly. (**a**) I-SceI-induced GFP$^+$ cells in *Xrcc4*$^{+/+}$ *versus* *Xrcc4*$^{-/-}$ sGEJ reporter mouse ES cells, as a function of time following transfection of I-SceI. The time point corresponding to 50% maximal GFP expression is shown in each case. (**b**) Ratio of I-SceI-induced GFP$^+$ cells in *Xrcc4*$^{+/+}$ *versus* *Xrcc4*$^{-/-}$ sGEJ reporter mouse ES cells, as a function of time following transfection of I-SceI. This ratio was calculated from the data shown in (**a**). (**c**) Percentage of I-SceI-induced GFP$^+$ cells in *Xrcc4*$^{-/-}$ sGEJ reporter mouse ES cells stably or transiently expressing empty vector or wild-type human *XRCC4*. Bars represent the mean of triplicates in a representative experiment. Error bars indicate s.e.m. Student's paired *t*-test (two-tailed) between *XRCC4 versus* empty vector, $P = 0.00027$ for stable and $P = 0.0001$ for transient. Steady state levels of XRCC4 protein are shown under the chart with β-actin as a loading control. The data indicates that expression of wild-type human *XRCC4* rescues NHEJ defective in *Xrcc4*$^{-/-}$ cells.

**Supplementary Figure 3**

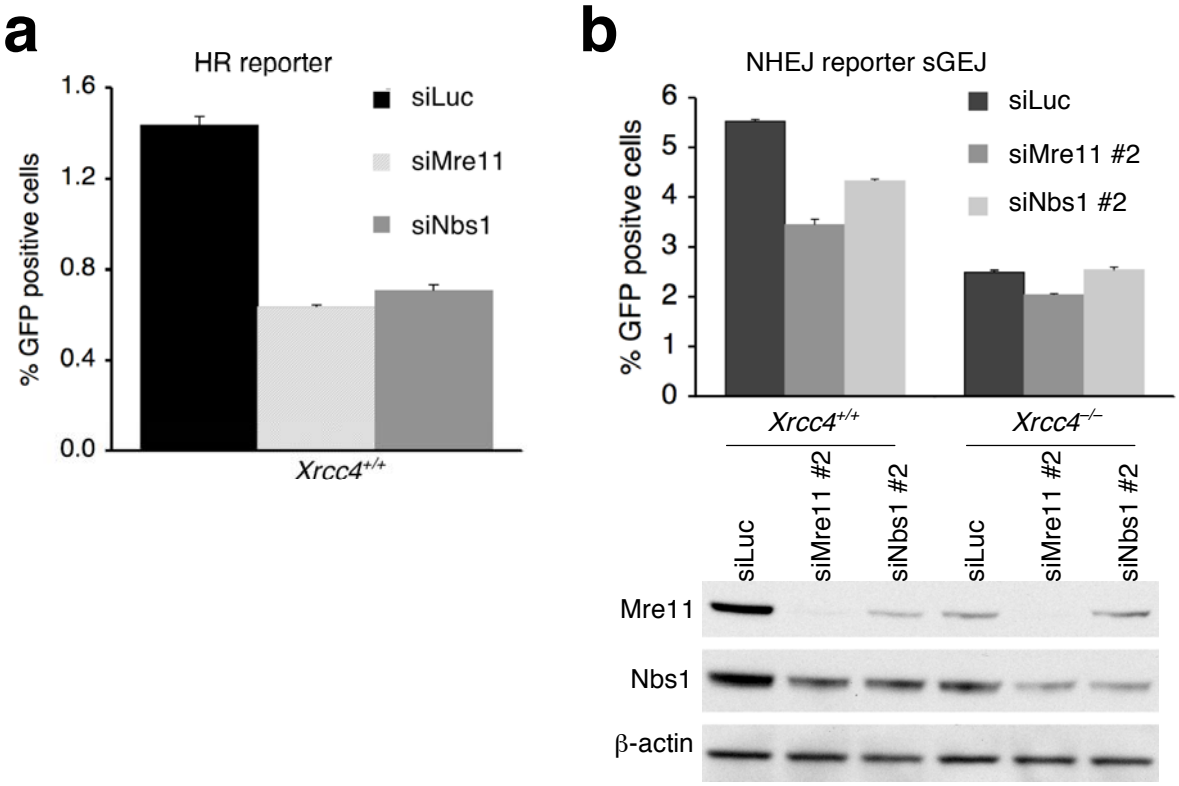


**Supplementary Figure 3** Mre11 regulates HR, *Xrcc4*-dependent NHEJ and *Xrcc4*-independent NHEJ. **(a**) Percentage of I-SceI-induced GFP$^+$ cells in *XRCC4*$^{+/+}$ mouse ES cells containing an HR/SCR reporter and co-transfected with siMre11, siNbs1 or control siLuc. Bars represent the mean of triplicates in a representative experiment. Error bars indicate s.e.m. Student's paired *t*-test (two-tailed): siMre11 *versus* siLuc, $P = 0.001$; siNbs1 *versus* siLuc, $P = 0.0058$. **(b**) Percentage of I-SceI-induced GFP$^+$ cells from *Xrcc4*$^{+/+}$ and *Xrcc4*$^{-/-}$ sGEJ reporter mouse ES cells depleted of Mre11 or Nbs1 by a second set of siRNA duplex (siMre11: acaggagaagagatcaact; siNbs1: gcagttgaatctaagaaac) with siLuc as a control. Bars represent mean of triplicates. Error bars indicate s.e.m. Student's paired *t*-test (two-tailed): in *Xrcc4*$^{+/+}$ cells, siMre11 *versus* siLuc, $P = 0.0012$; siNbs1 *versus* siLuc, $P = 0.00038$; in *Xrcc4*$^{-/-}$ cells, siMre11 *versus* siLuc, $P = 0.0166$; siNbs1 *versus* siLuc, not significant ($P = 0.704$). Protein abundance in these siRNA-treated *Xrcc4*$^{+/+}$ and *Xrcc4*$^{-/-}$ mouse ES cells was examined by Western blotting and is shown under the chart. β-actin serves as a loading control.

**Supplementary Figure 4**

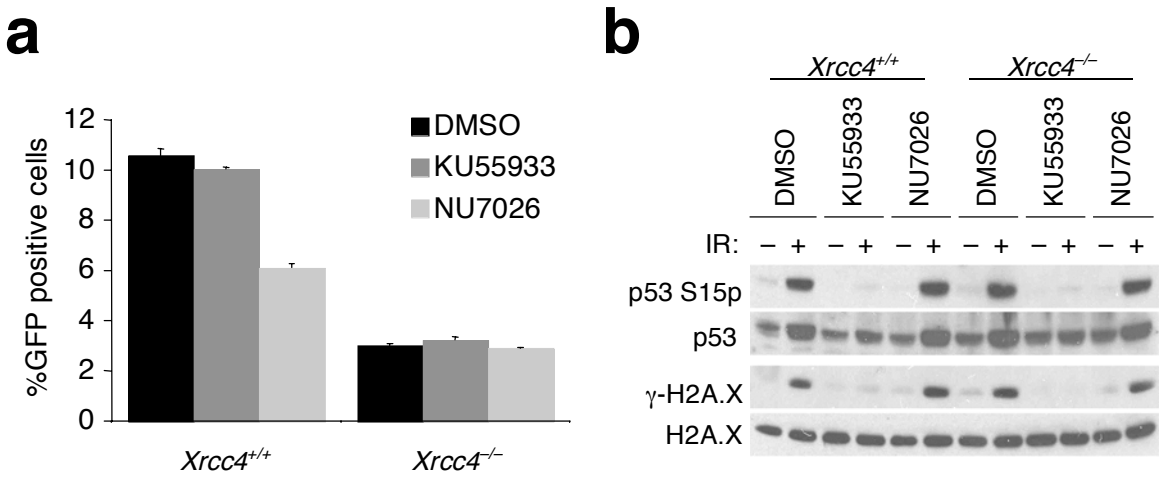


**Supplementary Figure 4** Atm inhibition has no effect on either *Xrcc4*-dependent NHEJ or *Xrcc4*-independent NHEJ. **(a)** Percentage of I-SceI-induced GFP$^{+}$ cells from *Xrcc4*$^{+/+}$ and *Xrcc4*$^{-/-}$ sGEJ reporter mouse ES cells treated with Atm inhibitor KU55933 and DNA-PKcs inhibitor NU7026. Bars represent mean of triplicates. Error bars indicate s.e.m. Student's paired *t*-test (two-tailed): in *Xrcc4*$^{+/+}$ cells, DMSO *versus* NU7026, $P = 0.002$; in *Xrcc4*$^{-/-}$ cells, DMSO *versus* NU7026, not significant ($P = 0.209$); in both cells, DMSO *versus* KU55933, not significant ($P = 0.242$ and $P = 0.309$ respectively). (**b**) Effect of KU55933 and NU7026 on phosphorylation of p53 Ser15 and H2A.X Ser139 in response to ionizing radiation (IR). *Xrcc4*$^{+/+}$ and *Xrcc4*$^{-/-}$ sGEJ reporter mouse ES cells were treated for 1 hr with DMSO, KU55933 (20 μM) or NU7026 (40 μM) followed by exposure to 5 Gy of IR. After 2 hrs, the cells were analyzed for p53 Ser15 phosphorylation (p53 S15p) and γ-H2A.X by Western blotting. Levels of p53 and H2A.X are shown as respective loading controls.

**Supplementary Figure 5**

**a**

NHEJ reporter sGEJ

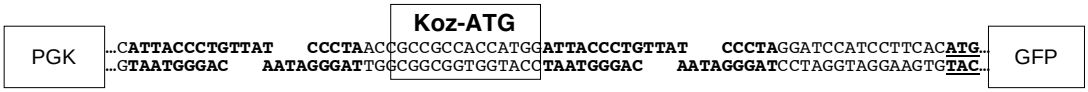


**b**

*Xrcc4*$^{+/+}$

siLuc

Accurate repair: 49 clones — I-SceI cutting

```
CATTACCCTGTTTAT  0nt  CCCTAGGATCCATCCTTCACATG  both (x49)
```

Deletion+michrohomology: 16 repair events

```
GATTACCCTGTT 1nt  TATCCCTAGGATCCATCCTTCACATG  2nd
GATTACCCTG  1nt  TATCCCTAGGATCCATCCTTCACATG  2nd
GATTACCCTGTTA  4nt  TAGGATCCATCCTTCNCATG  2nd
GATTACCCTG  7nt  TAGGATCCATCCTTCACATG  2nd  (x2)
CATTA  9nt  CCCTAGGATCCATCCTTCACATG  both (x3)
TTA 9nt CCCTAACCGCCGCCACCATGGGATTACC 28nt TG  both/1st
GATTA  9nt  CCCTAGGATCCATCCTTCACATG  2nd
CATTACCCTGTT  13nt  ATCCTTCACATG  both (x2)
GCCGCCA  20nt  CCTAGGATCCATCCTTCACATG  2nd
GATTACCCTGTT  25nt  ATCAGCAAGGGCGAGG  2nd
CATTACCCTGTTATCCCTAA  45nt  CACATG  2nd  (x2)
```

Deletion/no microhomology: 5 repair events

```
GATTACCCTG  4nt  CCCTAGGATCCATCCTTCACATG  2nd  (x2)
CATTACCCTG  9nt  GGATCCATCCTTCACATG  both
TTA 9nt CCCTAACCGCCGCCACCATGGGATTACC 28nt TG  both/2nd
CCG  79nt  TAGGATCCATCCTTCACATG  both
```

Deletion+insertion: 0 clone

Total: 69 clones/70 repair events

siMre11

Accurate repair: 48 clones — I-SceI cutting

```
CATTACCCTGTTTAT  0nt  CCCTAGGATCCATCCTTCACATG  both (x48)
```

Deletion+michrohomology: 9 clones

```
GATTACCCTGT  6nt  TAGGATCCATCCTTCACATG  2nd
GATTACCCTG  7nt  TAGGATCCATCCTTCACATG  2nd  (x3)
GATTACCCT  10nt  GGATCCATCCTTCACATG  2nd
CATTA  10nt  CCTAGGATCCATCCTTCACATG  both
CCCTAACCGCCGCCA 19nt CCCTAGGATCCATCCTTCACATG  2nd
GAATT  24nt  CATCCTTCACATG  both
GCCAGCT  53nt  CTAGGATCCATCCTTCACATG  both
```

Deletion/no microhomology: 8 clones

```
GATTACCCTGTTA  1nt  CCCTAGGATCCATCCTTCACATG  2nd  (x2)
GCCGCCACCATGGAT  16nt  GGATCCATCCTTCACATG  2nd
GATTACCCTG  4nt  CCCTAGGATCCATCCTTCACATG  2nd  (x5)
```

Deletion+insertion: 1 clone

```
CCCTAACCGCC  41nt (29nt)  ACATG  2nd
```

Total: 66 clones

**c**

*Xrcc4*$^{-/-}$

siLuc

Accurate repair: 5 clones — I-SceI cutting

```
CATTACCCTGTTTAT  0nt  CCCTAGGATCCATCCTTCACATG  both (x5)
```

Deletion+michrohomology: 35 clones

```
GATTACCCTGTTAT 1nt  ATCCCTAGGATCCATCCTTCACATG  2nd  (x2)
GATTACCCTGT  6nt  TAGGATCCATCCTTCACATG  2nd
GATTACCCTG  7nt  TAGGATCCATCCTTCACATG  2nd
CATTA  9nt  CCCTAGGATCCATCCTTCACATG  both (x2)
GATTA  9nt  CCCTAGGATCCATCCTTCACATG  2nd  (x2)
GATTA  10nt  CCTAGGATCCATCCTTCACATG  2nd  (x6)
GATTACCCT  10nt  GGATCCATCCTTCACATG  2nd  (x5)
CATTAC  17nt  CCATCCTTCACATG  both
GCCGCCA  20nt  CCTAGGATCCATCCTTCACATG  2nd  (x2)
GCCGCCACCAT  20nt  GGATCCATCCTTCACATG  2nd
ACCG  26nt  CCTAGGATCCATCCTTCACATG  2nd
GCCGCCACCATGGA  26nt  TCACATG  2nd
GCCGCCA  28nt  CCATCCTTCACATG  2nd  (x5)
CCCTAA  45nt  CACATG  2nd
GCCCAAGCTCTAG  48nt  CCTAGGATCCATCCTTCACATG  both (x2)
GCCCAAGC  51nt  TCCCTAGGATCCATCCTTCACATG  both
CCTTTCGA  66nt  CCCTAGGATCCATCCTTCACATG  both
```

Deletion/no microhomology: 3 clones

```
GATTACCCTGTTA  1nt  CCCTAGGATCCATCCTTCACATG  2nd  (x2)
CATTACC  14nt  ATCCATCCTTCACATG  both
```

Deletion+insertion: 3 clones

```
ATTACCCTG 2nt (1nt) ATCCCTAGGATCCATCCTTCACATG  2nd
CCCTAA  28nt (18nt)  CCCTAGGATCCATCCTTCACATG  2nd
CCCTAA  28nt (8nt)  CCCTAGGATCCATCCTTCACATG  2nd
```

Insertion: 3 clones

```
GATTACCCTGTT (2nt)  ATCCCTAGGATCCATCCTTCACATG  2nd
CATTACCCTGTTAT (8nt)  CCCTAGGATCCATCCTTCACATG  both
GATTACCCTGTTAT (29nt) CCCTAGGATCCATCCTTCACATG  2nd
```

Total: 49 clones

siMre11

Accurate repair: 8 clones — I-SceI cutting

```
CATTACCCTGTTTAT  0nt  CCCTAGGATCCATCCTTCACATG  both (x8)
```

Deletion+michrohomology: 44 clones

```
GATTACCCTGT  2nt  TCCCTAGGATCCATCCTTCACATG  2nd
CA  8nt  TTATCCCTAGGATCCATCCTTCACATG  both (x6)
CATTA  9nt  CCCTAGGATCCATCCTTCACATG  both (x3)
GATTA  9nt  CCCTAGGATCCATCCTTCACATG  2nd  (x2)
GATTACCCT  10nt  GGATCCATCCTTCACATG  2nd  (x7)
CATTACCCT  10nt  GGATCCATCCTTCACATG  both
GAT  10nt  TCCCTAGGATCCATCCTTCACATG  2nd  (x2)
GATTA  10nt  CCTAGGATCCATCCTTCACATG  2nd  (x2)
GATTACCCTGTT  13nt  ATCCTTCACATG  2nd  (x6)
CATTACCCTGTTAT  19nt  CATG  2nd
GCCGCCA  19nt  CCCTAGGATCCATCCTTCACATG  2nd
GCCGCCA  20nt  CCTAGGATCCATCCTTCACATG  2nd
ACCGCCG  23nt  CCTAGGATCCATCCTTCACATG  2nd  (x2)
GATTACCCTGTT  25nt  ATAG  2nd
GCCGCCA  28nt  CCATCCTTCACATG  2nd  (x3)
AAGCTTCGAA  31nt  TTCACATG  both
ACCGCCGCCAC  37nt  CATG  2nd
ACCG  38nt  CCTTCACATG  2nd  (x2)
GCCCAAGCTCTAG  47nt  CCCTAGGATCCATCCTTCACATG  both
```

Deletion/no microhomology: 6 clones

```
GATTACCCTGTTA  1nt  CCCTAGGATCCATCCTTCACATG  2nd  (x5)
GCCGCCACCATGGA  16nt  AGGATCCATCCTTCACATG  2nd
```

Deletion+insertion: 3 clones

```
ATTACCCT 5nt (17nt) ATCCCTAGGATCCATCCTTCACATG  2nd
GCCGCCACCATGGATTACC  35nt (4nt)  (ATGATCAG)C  2nd
TCTCGAGCTCCT  38nt (2nt)  TCCTTCACATG  both
```

Insertion: 3 clones

```
GATTACCCTG (2nt)  TTATCCCTAGGATCCATCCTTCACATG 2nd
GATTACCCTGTTATCCCTAGG (8nt)  ATCCATCCTTCACATG 2nd
GATTACCCTGTTAT (5nt)  CCCTAGGATCCATCCTTCACATG 2nd
```

Total: 64 clones

**Supplementary Figure 5** Analysis of repair junctions in cells lacking *Xrcc4* and cells depleted of Mre11. **(a)** Junction sequence of the NHEJ reporter sGEJ. The two I-SceI sites are in bold. Start codon of *GFP* ORF is in bold and underlined. The *PGK* (*phosphoglycerate kinase*) promoter and the *GFP* cDNA are indicated. (**b**, **c**) Junction sequences of I-SceI-induced $GFP^+$ repair products from $Xrcc4^{+/+}$ cells (**b**) and $Xrcc4^{-/-}$ cells (**c**) depleted of Mre11 by siMre11 in comparison with siLuc. Repair events are categorized as indicated. Tracts of microhomology are in bold and underlined. The number of deleted nucleotides is indicated in each repair event. Locations of I-SceI cutting within the NHEJ reporter are also shown followed by the number of identical repair junctions in parentheses.

**Supplementary Figure 6**

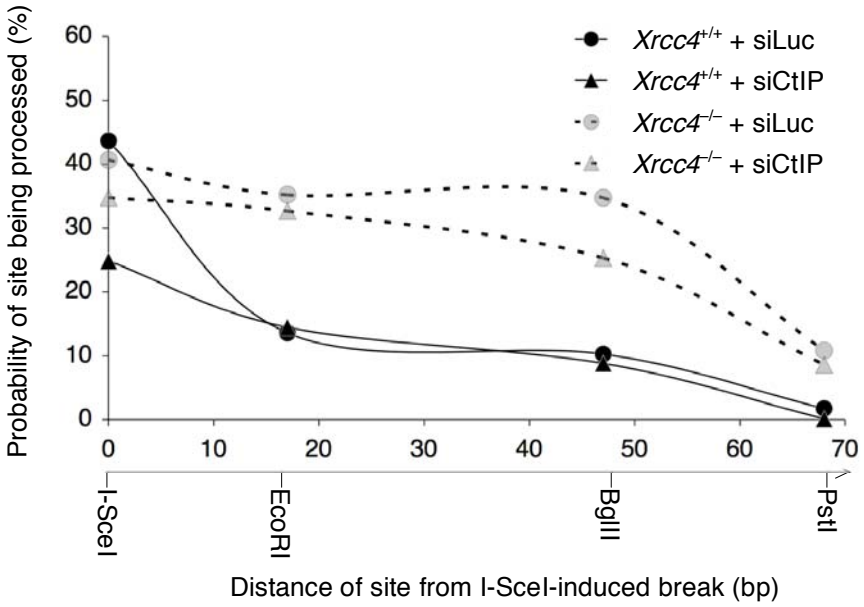


**Supplementary Figure 6** Effect of CtIP depletion on NHEJ-associated end processing. DNA bands in the Southern blot shown in **Figure 2b** were quantified by phosphoimager and densitometry. The probability of the restriction site being processed is calculated as the intensity of the "uncut" band divided by the combined intensities of "cut" and "uncut" bands (expressed as a percentage). The probability is plotted against the distance of each site from the I-SceI-induced break indicated along the *x*-axis.

**Supplementary Figure 7**

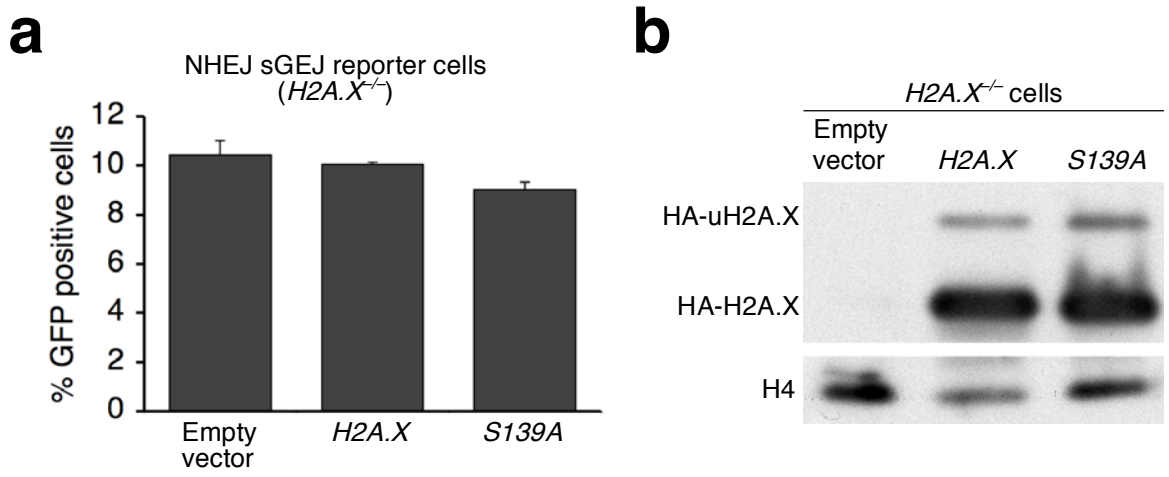


**Supplementary Figure 7** Expression of wild-type *H2A.X* has no effect on NHEJ in *H2A.X*$^{-/-}$ cells. (**a**) Percentage of I-SceI-induced GFP$^{+}$ cells in *H2A.X*$^{-/-}$ sGEJ reporter mouse ES cells transiently expressing either empty vector, HA-tagged wild-type *H2A.X* or *S139A* mutant alleles. Bars represent mean of triplicates. Error bars indicate s.e.m. Student's paired *t*-test between empty vector *versus* other samples, not significant (*versus* wild-type *H2A.X*, $P = 0.577$; *versus S139A*, $P = 0.204$). (**b**) Steady state levels of HA-tagged H2A.X and its S139A mutant proteins expressed in the *H2A.X*$^{-/-}$ sGEJ reporter mouse ES cells. HA-tagged H2A.X and mono-ubiquitinated HA-tagged H2A.X (HA-uH2A.X), as well as histone H4 as a loading control, are indicated.

**Supplementary Table 1** I-SceI cutting in I-SceI-induced NHEJ products

| | Number of repair events | | | | Percentage of all NHEJ events (%) | | | |
|---|---|---|---|---|---|---|---|---|
| | *Xrcc4*$^{+/+}$ | | *Xrcc4*$^{-/-}$ | | *Xrcc4*$^{+/+}$ | | *Xrcc4*$^{-/-}$ | |
| I-SceI cutting | siLuc | siMre11 | siLuc | siMre11 | siLuc | siMre11 | siLuc | siMre11 |
| both+Kozak popout | 57 | 51 | 14 | 22 | 82.6 | 77.3 | 28.6 | 34.4 |
| both+no Kozak popout | 1 | - | - | - | 1.4 | - | - | - |
| 1st I-SceI site only | - | - | - | - | - | - | - | - |
| 2nd I-SceI site only | 11 | 15 | 35 | 42 | 15.9 | 22.7 | 71.4 | 65.6 |
| Total sequences | 69 | 66 | 49 | 64 | 100.0 | 100.0 | 100.0 | 100.0 |